



## Study of pyrolysis of high density polyethylene in the open system and estimation of its capability for co-pyrolysis with lignite

IVAN KOJIĆ<sup>1</sup>, ACHIM BECHTEL<sup>2</sup>, FRIEDRICH KITTINGER<sup>3</sup>, NIKOLA STEVANOVIĆ<sup>4#</sup>, MARKO OBRADOVIĆ<sup>5</sup> and KSENIJA STOJANOVIĆ<sup>4#\*</sup>

<sup>1</sup>University of Belgrade, Innovation Center of the Faculty of Chemistry, Studentski trg 12–16,

11000 Belgrade, Serbia, <sup>2</sup>Montanuniversität Leoben, Department of Applied Geosciences and Geophysics, Peter Turner Strasse 5, A-8700 Leoben, Austria, <sup>3</sup>Montanuniversität Leoben,

Department of Product Engineering, Franz-Josef-Strasse 18, A-8700 Leoben, Austria,

<sup>4</sup>University of Belgrade, Faculty of Chemistry, Studentski trg 12–16, 11000 Belgrade, Serbia

and <sup>5</sup>University of Belgrade, Faculty of Mechanical Engineering, Kraljice Marije 16, 11000 Belgrade, Serbia

(Received 15 December 2017, revised 6 February, accepted 9 February 2018)

**Abstract:** Pyrolysis of high density polyethylene (HDPE) in the open system was studied. A plastic bag for food packing was used as a source of HDPE. Pyrolysis was performed at temperatures of 400, 450 and 500 °C, which were chosen based on thermogravimetric analysis. The HDPE pyrolysis yielded liquid, gaseous and solid products. Temperature rise resulted in the increase of conversion of HDPE into liquid and gaseous products. The main constituents of liquid pyrolysates are 1-n-alkenes, n-alkanes and terminal n-dienes. The composition of liquid products indicates that the performed pyrolysis of HDPE could not serve as a standalone operation for the production of gasoline or diesel, but preferably as a pre-treatment to yield a product to be blended into a refinery or petrochemical feed stream. The advantage of a liquid pyrolysate in comparison to crude oil is the extremely low content of aromatic hydrocarbons and the absence of polar compounds. The gaseous products have desirable composition and consist mainly of methane and ethene. The solid residues do not produce ash by combustion and have high calorific values. Co-pyrolysis of HDPE with mineral-rich lignite indicated positive synergetic effect at 450 and 500 °C, which is reflected through the increased experimental yields of liquid and gaseous products in comparison to theoretical ones.

**Keywords:** high density polyethylene; open pyrolysis system; TGA–FTIR; GC–MS; lignite; synergetic effect.

\* Corresponding author. E-mail: ksenija@chem.bg.ac.rs

# Serbian Chemical Society member.

<https://doi.org/10.2298/JSC171215027K>

## INTRODUCTION

The plastics are one of the most widely used materials. The plastics production has increased by an average of almost 10 % every year on a global basis since 1950.<sup>1</sup> High density polyethylene (HDPE) is the third largest produced plastic material in the world, after polyvinyl chloride and polypropylene, in terms of volume. It was estimated that 1.75 kg of petroleum (in terms of energy and raw materials) is necessary to make 1 kg of HDPE.<sup>2</sup>

The recycling of plastics and the conversion of polymeric materials into useful products, on the large scale, have been occurring for more than 20 years. The recycling of plastics could be performed *via* pyrolysis, hydrolysis, hydrogenation, methanolysis and gasification. The most attractive technique for the recycling of hydrocarbon polymers, such as HDPE, low density polyethylene and polypropylene is pyrolysis.<sup>1</sup> The pyrolysis process considers the thermal cracking of the polymeric material by heating in the absence of oxygen, which results in the formation of a solid residue (char), liquid product and gas. Yields of the products mainly depend on the pyrolysis temperature, the reactor type and the presence of catalysts. The pyrolysis of HDPE is usually conducted at temperatures between 400–600 °C. The most common catalysts used in this process are: zeolites, alumina, silica–alumina, fluid catalytic cracking (FCC) catalyst, reforming catalyst etc.<sup>1,2</sup> The usage of catalyst facilitates the degradation of HDPE at lower temperatures, even below 400 °C and changes reaction mechanism from radical into ionic.<sup>2–5</sup> Numerous studies provide the data regarding the optimized HDPE catalytic pyrolysis conditions, giving the highest yield of liquid or gaseous products. The brief overview of the literature data is given in the Supplementary material to this paper.

However, in recent years apart from the pyrolysis of waste HDPE alone, or in the mixture with other plastic waste material, its co-pyrolysis with oil shale and coal gained increasing attention.<sup>6–9</sup> Namely, the plastic materials, such as polyethylene and polypropylene can be the source of hydrogen, during the pyrolysis of hydrogen depleted natural products, such as coal. In that way the co-pyrolysis of HDPE and coal results in the balance of carbon and hydrogen contents, giving the opportunity to certain advantages of the co-pyrolysis process. However, the optimized conditions for catalytic pyrolysis of HDPE alone are not appropriate for the pyrolysis of coal. On the other hand it was proven that the pyrolysis of coal or oil shale in the closed system favours the secondary processes due to the retention of products in the reaction medium. The close contact and the interaction of primary pyrolysis products with each other, as well as with the hot particles for relatively long time (at least few hours) facilitate the secondary reactions, such as further thermal oil cracking, coking of oil vapour on carbon residue, as well as recombination, condensation and aromatisation processes.<sup>10–13</sup> This results in higher yields of gas and solid residue in the closed system. Addi-

tionally, the yield of the solid residue can be affected by the coke aggregates and its accumulation on the solid residue.<sup>10</sup> On the other hand, in the open system, the secondary processes occur less, because of the relatively short residence time of the primary generated products, that are being carried by an inert gas, and then immediately collected in a cold trap.<sup>14</sup> Recently, the pyrolysis in the open system has been proven as a method for significant thermal degradation of the following polymeric materials: carboxymethyl cellulose, hydroxyethyl cellulose, polyacrylamide and poly(vinylpyrrolidone) as well as for the accurate detection of their primary pyrolysis products.<sup>15–17</sup>

Considering that the pyrolysis of oil shale and coal in the open system prevents secondary processes, enabling higher yield of liquid products and that their co-pyrolysis with HDPE can be an attractive way to improve the conversion of these natural substrates into liquid products, as well as for the utilisation of waste HDPE, in the present paper pyrolysis of HDPE in the open system was studied in detail. Plastic bag for food packing was used as a source of HDPE. Its purity and thermal behavior was checked by elemental analysis and thermogravimetric analysis (TGA). Pyrolysis was performed at temperatures of 400, 450 and 500 °C. These temperatures were chosen based on TGA results. The solid residues were characterised by elemental analysis. The composition of liquid pyrolysis products was determined by the gas chromatography–mass spectrometry (GC–MS) technique, whereas the qualitative composition of gaseous products was estimated indirectly, based on Fourier transform infrared spectroscopy (FTIR) data from TGA. In order to compare the degradation behaviour of HDPE with cracking of kerogen from oil shale and coal in natural conditions, the stable carbon isotopic composition of the initial HDPE, solid and liquid pyrolysis products was measured. The possible application of obtained pyrolysis products has been proposed. Moreover, by co-pyrolysis of HDPE and mineral-rich lignite in the open system, positive synergetic effect at temperatures of 450 and 500 °C has been observed.

## EXPERIMENTAL

A plastic bag for food packing was used as the raw HDPE material.

Thermogravimetric analysis (TGA) was conducted using a Netzsch STA 449C instrument. 5.3 mg of sample was heated from 27 to 900 °C, at heating rate of 10 °C min<sup>-1</sup>. Nitrogen was used as the purge gas with the flow rate of 60 cm<sup>3</sup> min<sup>-1</sup>. The heating rate of 10 °C min<sup>-1</sup> was chosen, because at high heating rates, especially for endothermic reactions, the furnace temperature increases faster than the sample temperature, resulting in error of measurement, particularly when analysis is carried out in non-isothermal mode.<sup>18</sup> Fourier transform infrared spectroscopy (FTIR) was applied for the qualitative identification of generated gases, using ATI Matson Infinity Series FTIR instrument. The flow rate of nitrogen was chosen to optimize analysis of gases. TGA–FTIR analysis was done at the Department of Product Engineering, Montanuniversität Leoben, Austria, whereas other analyses were performed at the Faculty of Chemistry, University of Belgrade.

Pyrolysis of HDPE was performed in the open system (Carbolite tube furnace model MTF 10/15/130, UK) under a nitrogen atmosphere during 4 h at three temperatures: 400, 450 and 500 °C, with the heating rate of 5 °C min<sup>-1</sup>. The temperature range between 400 and 500 °C was chosen, based on the thermogravimetric properties of HDPE. The furnace (15 cm long) was equipped with a quartz tube (inner diameter 1 cm), which was 4.5 time longer than furnace. The quartz tube was situated within the furnace and the equal parts of the quartz tube were outside of furnace. The tube was connected with the nitrogen supply at the one side, while the other was connected with a trap (cooled to 0 °C), filled with 20 cm<sup>3</sup> of chloroform to which the pyrolysis products were transferred by the N<sub>2</sub> flow. The liquid products were collected in the cold trap, where the released gases could not be collected. The sample (1 g) was situated in the quartz vessel and the vessel with the sample was transferred into the pyrolysis furnace in the middle of the quartz tube.

The liquid product was extracted from the pyrolysis system using chloroform and combined with liquid product collected in the cold trap. Chloroform was removed by a rotary vacuum evaporator. The liquid product was dried to the constant mass at ambient conditions. The solid residue was dried in air and weighed, whereas yield of gas was calculated as: 100 % – (yield of liquid pyrolysate + yield of solid residue). Pyrolysis of HDPE at all three temperatures was performed 4 times and the average yields are reported here with standard deviations less than 0.5 %.

The liquid pyrolysis products obtained by the HDPE pyrolysis were analysed by gas chromatography–mass spectrometry (GC–MS). The detailed description of this analysis is given in the previous publications.<sup>13,19,20</sup>

The elemental analysis and the determination of ash content of the initial HDPE and the solid residues were performed according to the procedures which were explained in detail in the previous papers.<sup>20,21</sup>

For the determination of the carbon isotopic composition ( $\delta^{13}\text{C}$ ) of initial HDPE, liquid and solid pyrolysis products, 0.2–0.6 mg of sample was weighted using the microbalance (MX-5 ultramicrobalance, Mettler–Toledo, Giessen, Germany) and the sample was transferred into a small tin container (IVA Analysentechnik Meerbusch, Germany). The container was closed by tweezers. The capsules were placed in an autosampler (Thermo Scientific MAS 200R). A Flash EA 2000 HT elemental analyser was used, coupled to a Thermo Scientific Delta V Advantage isotope ratio mass spectrometer, *via* ConFlow IV Interface (He pressure: 80 kPa, CO<sub>2</sub> pressure: 200 kPa). The elemental analyser was operated in the NC (nitrogen–carbon) mode and controlled by the Isodat 3.0 software. Settings of elemental analyser were: reactor temperature 1020 °C, GC temperature 60 °C, carrier flow 100 cm<sup>3</sup> min<sup>-1</sup>, O<sub>2</sub> flow 250 cm<sup>3</sup> min<sup>-1</sup>, O<sub>2</sub> injection time 1 s and autosampler delay 16 s. The CO<sub>2</sub> reference gas pulse was introduced two times (20 s each) at the beginning of each run. The ConFlo interface (Thermo Scientific) diluted the CO<sub>2</sub> sample peak with helium in a split of 1:10. The CO<sub>2</sub> reference gas used to calculate the  $\delta^{13}\text{C}$  values in each analytical run was calibrated with a laboratory working standards (glucose monohydrate, acetanilide and aspartic acid), which were calibrated against certified reference materials (BCR-657 glucose and IAEA-600 caffeine). The Delta V Advantage (IRMS) mass spectrometer with a triple ion collector was used to simultaneously measure the signals at *m/z* 44, 45 and 46 of the molecular ions of the CO<sub>2</sub> formed by the sample combustion. One run took approximately 10 min. The stable isotope ratios are reported in delta notation ( $\delta^{13}\text{C}$ ) relative to the Pee Dee Belemnite (PDB) standard ( $\delta^{13}\text{C} = (^{13}\text{C}/^{12}\text{C})_{\text{sample}}/(^{13}\text{C}/^{12}\text{C})_{\text{standard}} - 1$ ). The delta notation is expressed in parts per thousand (‰).

In order to evaluate the synergetic effect between HDPE and the low rank coal, the pyrolysis of the mineral-rich lignite, originated from the Kostolac Basin<sup>20</sup> and its co-pyrolysis with HDPE in the mass ratio 1:1 (lignite/HDPE mixture) were also performed under the same conditions as for HDPE alone. Mineral-rich coal was chosen since this lithotype contains lower amount of organic matter than matrix- and xylite-rich coal.<sup>22,23</sup> Therefore, it allows to study of the influence of HDPE on the lowest quality low rank coal, by co-pyrolysis. As for the pyrolysis of HDPE alone, all experiments were repeated 4 times and the average yields are reported here with standard deviations less than 0.3 and 0.5 % for lignite and lignite/HDPE mixture, respectively.

## RESULTS AND DISCUSSION

### *Results of TGA analysis*

The purity and the thermal properties of plastic bag, which was used as a source of HDPE, were evaluated by TGA and elemental analysis (Fig. 1; Table I). Both analyses were in accordance with previously reported results.<sup>1,24</sup> TGA indicates that the thermal degradation of HDPE starts about 420 °C and almost finishes about 500 °C (Fig. 1). The differential scanning calorimetry (DSC) showed two main peaks (Fig. 1). The first peak at 130 °C corresponds to the melting of HDPE without the loss of mass. The second peak, associated with the mass loss, started at 390 °C and finished at 505 °C. The presence of a single peak in the derivative weight loss analysis (Fig. 1) indicates that there is only one degradation step in which the conversion takes place. The temperature of the maximum volatile matter releasing is 481.6 °C, and maximum rate of the volatile matter evolution of 33.52 % is observed at 483.6 °C. Temperatures for the open pyrolysis experiments were chosen based on TGA data. Although the appreciable mass loss at 400 °C was not recorded, the pyrolysis in the open system was performed at this temperature in order to check the influence of time (4 h at 400 °C versus only 6 s in TGA).

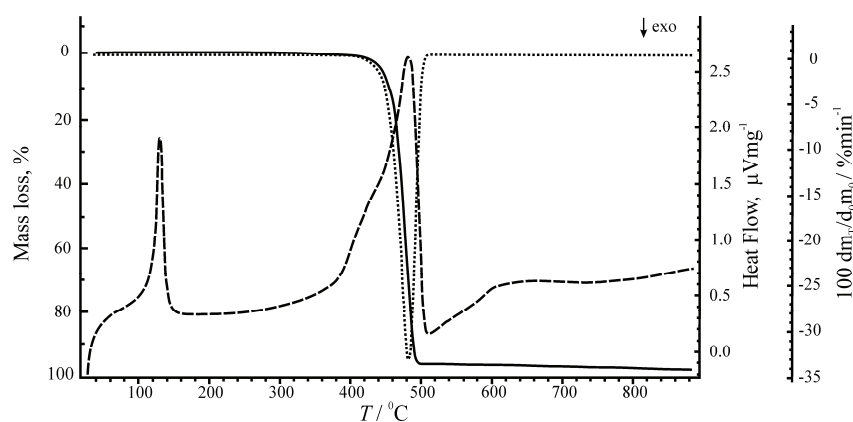


Fig. 1. The characteristic mass loss (TGA; full line), differential scanning calorimetry (DSC; dashed line) and derivative weight loss (DTG; dotty line) curve of HDPE.

TABLE I. Elemental analysis and molecular formulas of initial HDPE and solid pyrolysis products

Sample	C, %	H, %	O, %	Molecular formula
Initial HDPE	84.90	14.70	0.40	$\text{CH}_{2.08}\text{O}_{0.0035}$
Solid residue at 400 °C	86.22	13.60	0.18	$\text{CH}_{1.89}\text{O}_{0.0016}$
Solid residue at 450 °C	86.26	13.59	0.15	$\text{CH}_{1.89}\text{O}_{0.0013}$
Solid residue at 500 °C	86.37	13.55	0.08	$\text{CH}_{1.88}\text{O}_{0.0007}$

*Yields of the HDPE pyrolysis products*

The pyrolysis of HDPE in the open system yielded liquid (oil), gaseous and solid products. The distributions of these products are different at different temperatures and are shown in Table II.

TABLE II. Yields (%) of the pyrolysis products

Sample <i>t</i> / °C	HDPE			Lignite			Lignite/HDPE mixture		
	Liquid	Gas	Solid	Liquid	Gas	Solid	Liquid	Gas	Solid
400	12.96	7.41	79.63	1.11	16.02	82.87	7.49	11.37	81.14
450	21.32	11.51	67.17	1.19	19.82	78.99	15.79	21.08	63.13
500	33.94	15.77	50.29	1.20	20.08	78.72	23.95	40.01	36.04

As expected, the increase of the temperature from 400 to 500 °C resulted in the increase of HDPE conversion into liquid and gaseous products (Table II). The increase of oil yield, associated with the decrease of yield of the solid residue, was more pronounced between 450 and 500 °C than between 400 and 450 °C. This result is consistent with the results of TGA (Fig. 1). On the other hand, the increase of yield of gases between 400 and 450 °C, as well as between 450 and 500 °C was uniform, about 4 % (Table II). This result implies that the secondary process of the further thermal oil cracking into gas is avoided to the great extent in the open system pyrolysis.

*Carbon isotopic composition of initial HDPE, solid and liquid pyrolysis products*

The results of the carbon isotopic composition of initial HDPE, solid and liquid pyrolysis products (gases were not measured) are given in Table III. The initial HDPE has  $\delta^{13}\text{C}$  of  $-31.3\text{ ‰}$ . The liquid and the solid products at 400 °C are enriched in  $^{13}\text{C}$  in comparison to the initial HDPE. The content of  $^{13}\text{C}$  is higher in solid than in liquid product. This result indicates that the degradation of polymer in the open system pyrolysis follows the order of degradation of the carbon–carbon bonds in natural conditions, since the breaking of chemical bonds in which  $^{13}\text{C}$  isotope participates requires more energy than the breaking of  $^{12}\text{C}$ – $^{12}\text{C}$  bonds.<sup>25</sup> The increase of temperature from 400 to 450 °C results in further degradation of solid residue enriched in  $^{13}\text{C}$ , which is reflected through the increased content of  $^{13}\text{C}$  in liquid product (Table III). Moreover, by the temperature

increase to 450 °C the liquid product can be partly degraded to lighter gaseous products (enriched in  $^{12}\text{C}$ ), which also contributes to its  $^{13}\text{C}$  enrichment. The temperature increase from 450 to 500 °C is associated with further degradation of the solid product, whose yield decreased (Table II) and the production of liquid and gas. In accordance with the preferable cleavage of bonds where  $^{12}\text{C}$  participates, the enrichment of liquid product in  $^{12}\text{C}$  and the solid residue in  $^{13}\text{C}$  was observed (Table III). Data considering the isotopic compositions of HDPE and its pyrolysis products are scarce in literature. Despite the usage of different HDPE sources, our results are close to the reported  $\delta^{13}\text{C}$  data of the individual *n*-alkanes in liquid pyrolysates of HDPE at 500 °C, ~−30 ‰.<sup>26</sup>

TABLE III. Carbon isotopic composition ( $\delta^{13}\text{C}$  / ‰) of initial HDPE, liquid and solid pyrolysis products; initial HDPE: −31.30

Temperature, °C	Liquid	Solid residue
400	−31.03	−30.40
450	−30.88	−30.59
500	−30.96	−30.48

#### *The composition of liquid pyrolysis products*

The main constituents of all liquid pyrolysates of HDPE are terminal *n*-alkenes, *n*-alkanes and terminal *n*-dienes (Fig. S-1 of the Supplementary material; Table IV). These compounds are identified in range from C<sub>12</sub> to C<sub>43</sub>. Peaks of individual *n*-alkenes, *n*-alkanes and *n*-dienes can be accurately separated and integrated from the Total Ion Chromatogram (TIC) up to C<sub>27</sub> homologue. Therefore, the general composition of liquid pyrolysis products were firstly estimated based on the total abundances of C<sub>12</sub>–C<sub>43</sub> hydrocarbons, representing the sum of *n*-alkanes, 1-*n*-alkenes and terminal *n*-dienes, containing the same number of carbon atoms (Table IV).

The liquid pyrolysis product obtained at 400 °C is characterised by a broad maximum in range from C<sub>24</sub> to C<sub>32</sub> (Fig. S-1a; Table IV). The liquid pyrolysis product at 450 °C has almost equal abundances of C<sub>15</sub> to C<sub>33</sub> total hydrocarbons, whereas in liquid pyrolysate at 500 °C the most prominent are C<sub>15</sub>–C<sub>19</sub> hydrocarbons (Fig. S-1b, c; Table IV). This result suggests that in the open system pyrolysis at temperatures below 450 °C HDPE is mainly degraded into mid- to long-chain hydrocarbons, while above this temperature more intense cracking of mid- and long-chain intermediates occurs as well. This is consistent with the observation that lower molecular weight models of the normal chain unit are more stable than the initial polymer.<sup>2</sup> In all three liquid pyrolysates, the terminal *n*-alkenes in range C<sub>12</sub>–C<sub>27</sub> prevail over the corresponding *n*-alkanes and the terminal *n*-dienes, reaching the almost identical content of ≈51 %. The temperature increase from 400 to 500 °C resulted in the rise of *n*-diene content, associated with almost equal decrease in *n*-alkane abundance (Table IV).

TABLE IV. Percents of C<sub>12</sub>–C<sub>43</sub> total hydrocarbons (*n*-alkane + 1-*n*-alkene + terminal *n*-diene), percents of total C<sub>12</sub>–C<sub>27</sub> *n*-alkanes, 1-*n*-alkenes and terminal *n*-dienes and their ratios in liquid pyrolysates, calculated from TIC

Temperature, °C	Hydrocarbon										
	C <sub>12</sub>	C <sub>13</sub>	C <sub>14</sub>	C <sub>15</sub>	C <sub>16</sub>	C <sub>17</sub>	C <sub>18</sub>	C <sub>19</sub>	C <sub>20</sub>	C <sub>21</sub>	C <sub>22</sub>
400	1.10	2.02	2.73	3.23	3.43	3.52	3.61	3.59	3.81	3.72	4.06
450	1.80	2.72	3.52	3.99	4.01	4.07	4.04	4.01	3.90	3.73	3.94
500	0.24	1.74	3.59	4.70	4.90	5.12	5.27	5.06	4.81	4.29	4.29
Temperature, °C	C <sub>23</sub>	C <sub>24</sub>	C <sub>25</sub>	C <sub>26</sub>	C <sub>27</sub>	C <sub>28</sub>	C <sub>29</sub>	C <sub>30</sub>	C <sub>31</sub>	C <sub>32</sub>	C <sub>33</sub>
400	3.92	4.38	4.30	4.44	4.30	4.50	4.27	4.31	4.05	4.18	3.86
450	3.83	4.04	3.86	4.07	3.81	3.96	3.73	3.84	3.58	3.60	3.47
500	3.98	4.08	3.95	3.83	3.65	3.70	3.44	3.44	3.11	3.21	2.94
Temperature, °C	C <sub>34</sub>	C <sub>35</sub>	C <sub>36</sub>	C <sub>37</sub>	C <sub>38</sub>	C <sub>39</sub>	C <sub>40</sub>	C <sub>41</sub>	C <sub>42</sub>	C <sub>43</sub>	
400	3.69	3.15	2.82	2.15	1.54	1.40	1.01	0.98	1.33	0.63	
450	3.44	2.92	2.47	2.17	1.85	1.46	1.32	1.16	0.93	0.75	
500	2.84	2.51	2.21	1.91	1.74	1.43	1.18	0.96	1.21	0.68	
Total C <sub>12</sub> –C <sub>27</sub> <sup>a</sup> <i>n</i> -alkanes, 1- <i>n</i> -alkenes and terminal <i>n</i> -dienes, %						Ratios of sum of C <sub>12</sub> –C <sub>27</sub> homologues					
Temperature, °C	<i>n</i> -Alkanes	1- <i>n</i> -Alkenes	Terminal <i>n</i> -dienes	1- <i>n</i> -Alkenes/ <i>n</i> -alkanes	Terminal <i>n</i> -dienes/ 1- <i>n</i> -alkenes	Terminal <i>n</i> -dienes/ <i>n</i> -alkanes					
400	40.95	51.38	7.66	1.25	0.15	0.19					
450	37.73	51.50	10.77	1.37	0.21	0.29					
500	35.00	51.50	13.50	1.47	0.26	0.39					

<sup>a</sup>C<sub>x</sub> designates *n*-alkane, 1-*n*-alkene or terminal *n*-diene homologue, and x represents number of carbon atoms

The application of typical ion fragmentogram *m/z* 71 enabled the accurate separation and the integration of *n*-alkane peaks of up to C<sub>32</sub>. The liquid pyrolysis product obtained at 400 °C is characterised by the predominance of mid- and long-chain C<sub>23</sub> to C<sub>32</sub> *n*-alkanes over lower homologues (C<sub>12</sub>–C<sub>22</sub>), with the broad maximum in range from C<sub>24</sub> to C<sub>28</sub>. The liquid pyrolysis product at 450 °C has almost uniform contents of C<sub>12</sub> to C<sub>32</sub> *n*-alkanes, whereas in the pyrolysate at 500 °C the prevalence of lower homologues (C<sub>12</sub>–C<sub>22</sub>) is obvious, with maxima in C<sub>15</sub>–C<sub>18</sub> range (Fig. 2a). The liquid pyrolysis product obtained at 500 °C has the distribution of *n*-alkanes similar to those typical of terrestrial oil.<sup>25</sup> The contents of short- (C<sub>12</sub>–C<sub>18</sub>), mid- (C<sub>19</sub>–C<sub>25</sub>) and long-chain (C<sub>26</sub>–C<sub>32</sub>) homologues indicate that the temperature rise is mainly reflected through the decrease of long-chain homologues, associated with the increase of short-chain *n*-alkanes, whereas the abundance of the mid-chain homologues remains almost constant (Fig. 2; Table V).

The average chain length (ACL) showed a slight decrease with the temperature rise (Table V). The carbon preference index (CPI)<sup>27</sup> values, representing the ratios of odd versus even *n*-alkanes are close to 1, in whole range of *n*-alkanes (C<sub>12</sub>–C<sub>32</sub>), as well as for short- (C<sub>12</sub>–C<sub>18</sub>), mid- (C<sub>19</sub>–C<sub>25</sub>) and long-chain (C<sub>26</sub>–C<sub>32</sub>) homologues, independently of the pyrolysis temperature. However, a slight

predominance of the odd homologues is observed for short-chain homologues, C<sub>12</sub>–C<sub>18</sub> (Table V).

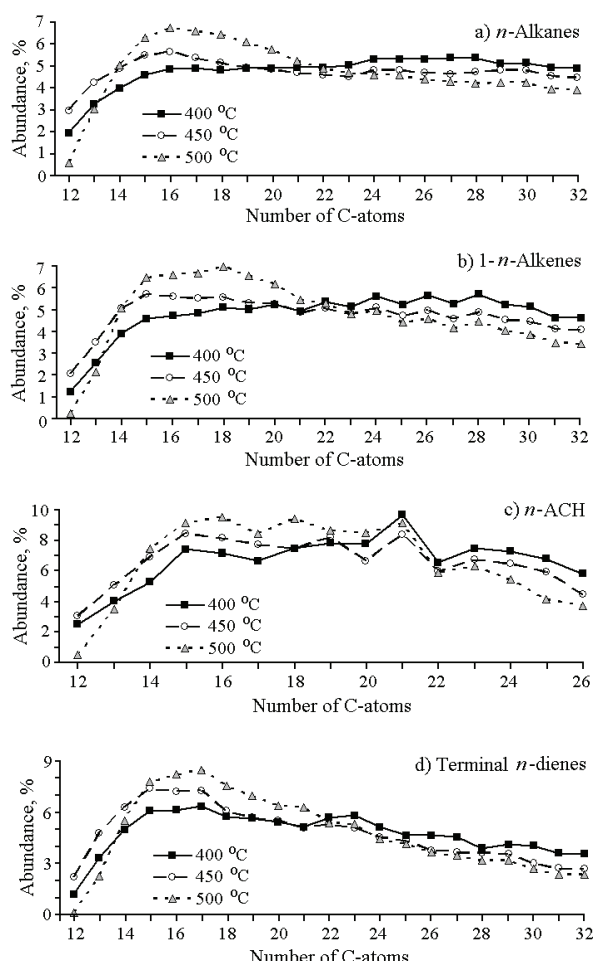


Fig. 2. Distributions of individual C<sub>12</sub>–C<sub>32</sub> *n*-alkanes (a), C<sub>12</sub>–C<sub>32</sub> 1-*n*-alkenes (b), C<sub>12</sub>–C<sub>26</sub> *n*-alkylcyclohexanes, *n*-ACH (c) and C<sub>12</sub>–C<sub>32</sub> terminal *n*-dienes (d) in liquid pyrolysates.

The distribution of terminal *n*-alkenes was studied using typical *m/z* 83 fragmentogram ion, allowing the accurate separation and the integration of peaks of up to C<sub>32</sub>. Distributions of terminal *n*-alkenes in liquid pyrolysates, at all three temperatures, are very similar to the distributions of *n*-alkanes (Fig. 2a, b), having almost identical ACL and CPI values (Table V). This result suggests that these two types of hydrocarbons were formed via the same radical reaction processes, consistent with the presence of a single peak in the derivative weight loss analysis (Fig. 1).

TABLE V. Parameters calculated from distributions of individual *n*-alkanes (*m/z* 71), 1-*n*-alkenes (*m/z* 83), *n*-alkylcyclohexanes (*m/z* 83) and terminal *n*-dienes (*m/z* 81) in liquid pyrolysates

<i>n</i> -Alkanes										
<i>t</i> / °C	C <sub>12</sub> –C <sub>18</sub>	C <sub>19</sub> –C <sub>25</sub>	C <sub>26</sub> –C <sub>32</sub>	ACL <sup>a</sup>	ACL	ACL	CPI <sup>b</sup>	CPI <sup>c</sup>	CPI <sup>d</sup>	CPI <sup>e</sup>
%	%	%	C <sub>12</sub> –C <sub>18</sub>	C <sub>19</sub> –C <sub>25</sub>	C <sub>26</sub> –C <sub>32</sub>	C <sub>12</sub> –C <sub>32</sub>	C <sub>12</sub> –C <sub>18</sub>	C <sub>19</sub> –C <sub>25</sub>	C <sub>26</sub> –C <sub>32</sub>	
400	28.43	35.39	36.18	15.45	22.06	28.93	1.01	1.06	1.00	0.99
450	33.89	33.34	32.77	15.28	21.98	28.98	1.01	1.04	0.99	1.00
500	34.76	35.90	29.34	15.76	21.79	28.93	1.01	1.08	1.00	0.99
1- <i>n</i> -Alkenes										
<i>t</i> / °C	C <sub>12</sub> –C <sub>18</sub>	C <sub>19</sub> –C <sub>25</sub>	C <sub>26</sub> –C <sub>32</sub>	ACL	ACL	ACL	CPI	CPI	CPI	CPI
%	%	%	C <sub>12</sub> –C <sub>18</sub>	C <sub>19</sub> –C <sub>25</sub>	C <sub>26</sub> –C <sub>32</sub>	C <sub>12</sub> –C <sub>32</sub>	C <sub>12</sub> –C <sub>1</sub> )	(C <sub>19</sub> –C <sub>25</sub> )	C <sub>26</sub> –C <sub>32</sub>	
400	27.06	36.57	36.38	15.63	22.05	28.86	0.96	1.04	0.94	0.95
450	33.16	35.21	31.63	15.46	21.94	28.87	0.97	1.03	0.95	0.95
500	34.20	37.75	28.04	15.90	21.75	28.80	0.97	1.05	0.96	0.95
<i>n</i> -Alkylcyclohexanes										
<i>t</i> / °C	C <sub>12</sub> –C <sub>16</sub>	C <sub>17</sub> –C <sub>21</sub>	C <sub>22</sub> –C <sub>26</sub>	ACL	ACL	ACL	CPI <sup>f</sup>	CPI <sup>g</sup>	CPI <sup>h</sup>	CPI <sup>i</sup>
%	%	%	C <sub>12</sub> –C <sub>16</sub>	C <sub>17</sub> –C <sub>21</sub>	C <sub>22</sub> –C <sub>26</sub>	C <sub>12</sub> –C <sub>26</sub>	C <sub>12</sub> –C <sub>16</sub>	C <sub>17</sub> –C <sub>21</sub>	C <sub>22</sub> –C <sub>26</sub>	
400	26.38	39.55	34.07	14.48	19.16	23.94	1.09	1.20	1.10	1.06
450	31.74	38.55	29.71	14.43	19.02	23.87	1.11	1.13	1.15	1.08
500	30.20	44.22	25.58	14.79	19.01	23.75	1.02	1.16	1.02	1.04
Terminal <i>n</i> -dienes										
<i>t</i> / °C	C <sub>12</sub> –C <sub>18</sub>	C <sub>19</sub> –C <sub>25</sub>	C <sub>26</sub> –C <sub>32</sub>	ACL	ACL	ACL	CPI	CPI	CPI	CPI
%	%	%	C <sub>12</sub> –C <sub>18</sub>	C <sub>19</sub> –C <sub>25</sub>	C <sub>26</sub> –C <sub>32</sub>	C <sub>12</sub> –C <sub>32</sub>	C <sub>12</sub> –C <sub>18</sub>	C <sub>19</sub> –C <sub>25</sub>	C <sub>26</sub> –C <sub>32</sub>	
400	33.97	37.58	28.45	15.62	21.92	28.82	1.02	1.11	0.99	1.02
450	41.31	35.65	23.04	15.42	21.83	28.75	1.04	1.11	1.00	1.01
500	40.07	39.01	20.92	15.94	21.66	28.68	1.04	1.10	1.05	1.02

<sup>a</sup>ACL – Average chain length; CPI – carbon preference index determined for distributions of *n*-alkanes, 1-*n*-alkenes, *n*-alkylcyclohexanes and terminal *n*-dienes; <sup>b</sup>CPI (C<sub>12</sub>–C<sub>32</sub>) = 1/2x[Σodd (C<sub>13</sub>–C<sub>31</sub>)/Σeven (C<sub>12</sub>–C<sub>30</sub>) + Σodd (C<sub>13</sub>–C<sub>31</sub>)/Σeven (C<sub>14</sub>–C<sub>32</sub>)]; <sup>c</sup>CPI (C<sub>12</sub>–C<sub>18</sub>) = 1/2x[Σodd (C<sub>13</sub>–C<sub>17</sub>)/Σeven (C<sub>12</sub>–C<sub>16</sub>) + Σodd (C<sub>13</sub>–C<sub>17</sub>)/Σeven (C<sub>14</sub>–C<sub>18</sub>)]; <sup>d</sup>CPI (C<sub>19</sub>–C<sub>25</sub>) = 1/2x[Σodd (C<sub>19</sub>–C<sub>25</sub>)/Σeven (C<sub>18</sub>–C<sub>24</sub>) + Σodd (C<sub>19</sub>–C<sub>25</sub>)/Σeven (C<sub>20</sub>–C<sub>26</sub>)]; <sup>e</sup>CPI (C<sub>26</sub>–C<sub>32</sub>) = 1/2x[Σodd (C<sub>27</sub>–C<sub>31</sub>)/Σeven (C<sub>26</sub>–C<sub>30</sub>) + Σodd (C<sub>27</sub>–C<sub>31</sub>)/Σeven (C<sub>28</sub>–C<sub>32</sub>)]; <sup>f</sup>CPI (C<sub>12</sub>–C<sub>26</sub>) = 1/2x[Σodd (C<sub>13</sub>–C<sub>25</sub>)/Σeven (C<sub>12</sub>–C<sub>24</sub>) + Σodd (C<sub>13</sub>–C<sub>25</sub>)/Σeven (C<sub>14</sub>–C<sub>26</sub>)]; <sup>g</sup>CPI (C<sub>12</sub>–C<sub>16</sub>) = 1/2x[Σodd (C<sub>13</sub>–C<sub>15</sub>)/Σeven (C<sub>12</sub>–C<sub>14</sub>) + Σodd (C<sub>13</sub>–C<sub>15</sub>)/Σeven (C<sub>14</sub>–C<sub>16</sub>)]; <sup>h</sup>CPI (C<sub>17</sub>–C<sub>21</sub>) = 1/2x[Σodd (C<sub>17</sub>–C<sub>21</sub>)/Σeven (C<sub>16</sub>–C<sub>20</sub>) + Σodd (C<sub>17</sub>–C<sub>21</sub>)/Σeven (C<sub>18</sub>–C<sub>22</sub>)]; <sup>i</sup>CPI (C<sub>22</sub>–C<sub>26</sub>) = 1/2x[Σodd (C<sub>23</sub>–C<sub>25</sub>)/Σeven (C<sub>22</sub>–C<sub>24</sub>) + Σodd (C<sub>23</sub>–C<sub>25</sub>)/Σeven (C<sub>24</sub>–C<sub>26</sub>)]; C<sub>x</sub> designates *n*-alkane, 1-*n*-alkene, *n*-alkylcyclohexane or terminal *n*-diene homologue, and x represents total number of carbon atoms

The detailed inspection of *m/z* 83 fragmentogram ion allowed us to identify *n*-alkylcyclohexanes ranging from C<sub>12</sub> to C<sub>26</sub> (total number of carbon atoms; Fig. 2c), however in much lower abundance in comparison to *n*-alkanes, *n*-alkenes and *n*-dienes. The presence of *n*-alkylcyclohexanes in all pyrolysates indicates the cyclisation of alkyl-radicals during pyrolysis. The ratio of total *n*-alkylcyclohexanes to total 1-*n*-alkenes, calculated from *m/z* 83 fragmentogram is relatively uniform, ~ 0.03, showing slight increase from 400 to 450 °C and then slight decrease from 450 to 500 °C. The distributions of *n*-alkylcyclohexanes are similar in all pyrolysates, showing maxima at C<sub>21</sub> (Fig. 2c). This result could be explained

by the fact that the long-chain radicals ( $> C_{25}$ ) have been more easily cracked than cyclised, since lower molecular weight normal chain units are more stable than the longer ones.<sup>2</sup> During pyrolysis, the content of long-chain radicals decreases, whereas the contents of mid- and short-chain ones increase. Mid- and short-chain radicals undergo further cracking, but in low extent they cyclise forming mainly alkylcyclohexanes, as in natural conditions (bitumen and crude oil).<sup>25,28</sup> With the increasing thermal stress, cracking is favoured which is documented by the additional *n*-alkylcyclohexane maxima at  $C_{19}$ , and  $C_{16}$ ,  $C_{18}$  (Fig. 2c) in pyrolysates obtained at temperatures of 450 and 500 °C, respectively.

*ACL* shows slight decrease with temperature rise, whereas *CPI* values indicate slight predominance of odd over even homologues particularly in short homologues range ( $C_{12}$ – $C_{16}$ , Table V). Distributions of *n*-alkylcyclohexanes at 450 and 500 °C showed difference in comparison to distributions of *n*-alkanes and 1-*n*-alkenes, which reflects through the increased content of mid-chain- and a slight decrease of short-chain homologues (Table V).

Distributions of terminal *n*-dienes were studied using typical *m/z* 81 ion fragmentogram, which enabled the accurate separation and integration of peaks up to  $C_{32}$ . The liquid pyrolysis product obtained at 400 °C is characterised by the relatively uniform abundance of all homologues, and in difference to *n*-alkanes and *n*-alkenes no prevalence of higher over lower homologues is observed (Fig. 2d). Liquid pyrolysis products at 450 and 500 °C have higher content of shorter homologues, particularly the latter one. Distributions of short- ( $C_{12}$ – $C_{18}$ ), mid- ( $C_{19}$ – $C_{25}$ ) and long-chain ( $C_{26}$ – $C_{32}$ ) dienes in pyrolysates at 450 and 500 °C show similarity with the distributions of *n*-alkylcyclohexanes, which reflects through the increase in content of mid- and slight decrease in short-chain homologues (Table V). *ACL* values are similar to those for *n*-alkanes and terminal *n*-alkenes, indicating that all three types of hydrocarbons are formed in the same type of radical processes. *CPI* values are very close to 1, however as in previous cases slight predominance of odd over even homologues is observed for the short-chain  $C_{12}$ – $C_{18}$  dienes (Table V).

The liquid pyrolysates contained very low amount of aromatic hydrocarbons. *n*-Alkylbenzenes (*m/z* 92) and *n*-alkyltoluenes (*m/z* 105) represent the exclusive aromatics found in HDPE pyrolysates, however in traces which avoided their integration and quantification. These compounds have been formed *via* dehydrocyclisation of reactive radicals. However, in the open system, short time of remaining and fast releasing of the primary pyrolysis products from the reaction medium by an inert gas disable secondary processes, including the formation of aromatic compounds, which resulted in their trace content.

The above mentioned discussion implies that HDPE can be converted into valuable liquid product by pyrolysis in the open system. This is particularly related to the pyrolysate obtained at 500 °C, which has *n*-alkane distribution similar

to crude oil of terrestrial origin (Figs. S-1c and 2a).<sup>25</sup> Pyrolysate at 450 °C has the *n*-alkane distribution similar to the immature crude oil of terrestrial origin (Figs. S-1b and 2a). The pyrolysate obtained at 400 °C is characterised by the prevalence of waxy hydrocarbons (Figs. S-1a and 2a), which indicates that under the applied conditions this temperature is not sufficient for the producing of liquid product, having the composition of *n*-alkanes similar to crude oil. This is consistent with the results of TGA analysis (Fig. 1), which showed negligible degradation of HDPE at 400 °C. Considering that by pyrolysis HDPE was exposed to heating at 400 °C for 4 h, in difference to TGA (6 s), however without significant degradation, the conclusion can be drawn that temperature has much more influence on the degradation process than the time of exposure to the particular temperature. This behaviour is similar to the behaviour of kerogen (insoluble organic matter in coal, oil shale and source rocks) during natural maturity processes.<sup>29</sup> The presence of reactive *n*-alkenes and *n*-dienes in liquid pyrolysates is desirable, since these hydrocarbons can be more easily converted into branched and cyclic hydrocarbons than *n*-alkanes, *via* reforming processes, therefore giving the opportunity for producing the high-octane gasoline. On the other hand, terminal *n*-alkenes, which can be isolated, are highly required in petrochemical industry where they are used as chemical feedstock for plastic and detergent manufacture.<sup>30</sup>

The obtained results showed that the pyrolysis of HDPE in an open system could not serve as a standalone operation for producing of gasoline or diesel, but preferably as a pretreatment to yield a product which is to be blended into a refinery or a petrochemical feed stream. The important environmental characteristic of liquid pyrolysate in comparison to crude oils is the extremely low content of aromatic hydrocarbons, the absence of undesirable organosulphur compounds, as well as the absence of asphaltenes and polar compounds which requires vacuum distillation.

#### *The composition of gaseous products*

Gaseous products produced in the open system pyrolysis could not been analysed. However the qualitative composition of gases was estimated based on TGA coupled to Fourier transform infrared spectroscopy (FTIR), Fig. 3.<sup>31,32</sup>

The gaseous products of HDPE destruction are light alkane and alkene hydrocarbons. The presence of gaseous alkanes is documented by the peaks around 2950 cm<sup>-1</sup>, representing C–H stretching and the peaks around 1370 cm<sup>-1</sup>, representing C–H scissoring and bending (Fig. 3). Gaseous alkenes are represented by peaks at around 3100 cm<sup>-1</sup>, corresponding to C–H stretching, peaks around 1450 cm<sup>-1</sup> corresponding to C=C stretching, as well as by peaks observed around 910 cm<sup>-1</sup> corresponding to C–H bending (Fig. 3). Much more pronounced peaks of C–H than of C–C or C=C vibrations indicate that the main gaseous products are

methane and ethene. The production of CO<sub>2</sub> (peaks between 2300 and 2400 cm<sup>-1</sup> corresponding to C=O stretching) can be explained by the presence of the minor amount of oxygen in initial HDPE (Table V), most probably originating from the additives which are intercalated to improve the properties of HDPE.<sup>33</sup> The further reaction of released CO<sub>2</sub> with hydrocarbons at high temperatures (above 850 °C) resulted in the formation of CO, whose presence is documented by peaks between 2100 and 2200 cm<sup>-1</sup>, representing C–O stretching (Fig. 3). The obtained result suggests that the pyrolysis of HDPE produces valuable gaseous products, rich in methane and ethene.

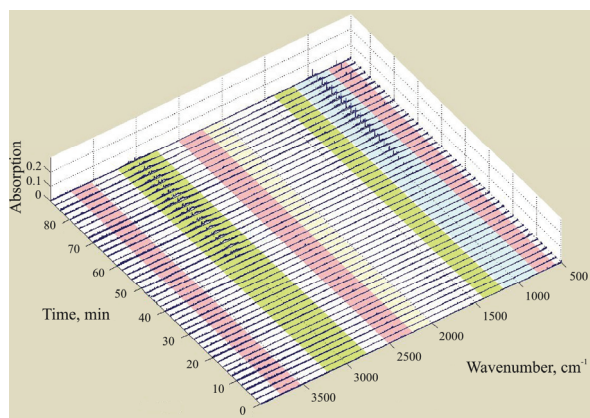


Fig. 3. TGA–FTIR thermogram of HDPE representing absorbance with respect to time and wavenumber. A time of 20 min corresponds to a temperature of 227 °C, 40 min to 427 °C, 60 min to 627 °C, 80 min to 827 °C. The ramp rate was 10 °C min<sup>-1</sup>.

#### *The composition of solid pyrolysis products*

The results of elemental analysis and the corresponding calculated molecular formulae of initial HDPE and solid residues are given in Table I. The solid residues at all temperatures are slightly depleted in hydrogen in comparison to the initial HDPE, which is expected due to the releasing of *n*-alkanes into liquid pyrolysate and methane into gas, which are enriched in hydrogen. The initial HDPE and solid residues at all three temperatures do not produce ash by combustion.

The calculated net calorific value based on 9 formulas proposed for hydrocarbon fuels and waste material (including plastic)<sup>34–41</sup> of the initial HDPE and the solid residues ranged from 38.91 to 46.74 MJ kg<sup>-1</sup> (Table VI) and is in agreement with reports from literature.<sup>1,30,42–44</sup> The calorific value of the initial HDPE and the solid pyrolysis products is higher than those of bituminous coal and petroleum coke.<sup>44,45</sup>

Despite the high net calorific values, it can be supposed that the solid residues have undesirable combustion behaviour, due to the melting during combustion. In order to modify the combustion behaviour of the solid residues, its mixing with biomass or coal was suggested. Namely the mixing of coal or bio-

mass with plastic residues can have a stabilizing effect on the plastic residues morphology and can prevent its melting during combustion.<sup>46</sup> Based on the obtained results, the mixing of solid residues with coal or biomass for combustion process has advantage, since the solid materials obtained by HDPE pyrolysis do not contain sulphur and do not produce ash by combustion.

TABLE VI. Calculated net calorific values (MJ kg<sup>-1</sup>) of initial HDPE and solid pyrolysis products

Sample	$Q_{n1}^a$	$Q_{n2}$	$Q_{n3}$	$Q_{n4}$	$Q_{n5}$	$Q_{n6}$	$Q_{n7}$	$Q_{n8}$	$Q_{n9}$
Initial HDPE	44.25	46.74	46.59	44.71	46.61	42.09	39.30	42.36	43.69
Solid residue at 400 °C	43.84	45.88	45.73	43.96	45.75	41.87	38.91	41.76	43.15
Solid residue at 450 °C	43.85	45.89	45.73	43.97	45.75	41.90	38.91	41.77	43.15
Solid residue at 500 °C	43.87	45.89	45.73	43.97	45.75	41.98	38.93	41.77	43.16

<sup>a</sup> $Q_n$  – Net calorific value;  $Q_{n1} = 38.2 \times$  mass proportion of C + 84.9 x (mass proportion of H – mass proportion of O/8) – 0.62;<sup>34</sup>  $Q_{n2} = 34.1 \times$  mass proportion of C + 121.4 x mass proportion of H – 15.3 x mass proportion of O + 10.5 x mass proportion of S;<sup>34</sup>  $Q_{n3} = 33.9 \times$  mass proportion of C + 121.5 x mass proportion of H – 12.7 x mass proportion of O + 9.3 x mass proportion of S;<sup>34</sup>  $Q_{n4} = 33.4 \times$  mass proportion of C + 117.7 x mass proportion of H – 15.6 x mass proportion of O;<sup>35</sup>  $Q_{n5} = 33.8 \times$  mass proportion of C + 122.3 x (mass proportion of H – mass proportion of O/8) + 9.4 x mass proportion of S;<sup>36</sup>  $Q_{n6} = (106.4 + 0.149 \times$  mass proportion of O) x (mass proportion of C/3 + mass proportion of H – mass proportion of O/8 + mass proportion of S/8) – 22.0 x mass proportion of H;<sup>37</sup>  $Q_{n7} = (1.52 \times$  mass proportion of H + 98.8) x (mass proportion of C/3 + mass proportion of H – mass proportion of O/8 + mass proportion of S/8) – 22.0 x mass proportion of H;<sup>38</sup>  $Q_g$  – Gross calorific value;  $Q_{g8} = 33 \times$  mass proportion of C + 120 x mass proportion of H – 16 x mass proportion of O;<sup>39</sup>  $Q_{g9} = 35.2 \times$  mass proportion of C + 116.2 x mass proportion of H + 6.3 x mass proportion of N + 10.5 x mass proportion of S – 11.1 x mass proportion of O;<sup>40,41</sup>  $Q_n = Q_g - 21.96 \times$  mass proportion of H<sup>34,42</sup>

#### *Co-pyrolysis of mineral-rich lignite and HDPE in the open system*

As for HDPE, rise of the temperature resulted in the increase of conversion of both lignite and lignite/HDPE mixture into liquid and gaseous products. However, the increase is much more prominent for HDPE and lignite/HDPE mixture, than for lignite alone (Table II).

The evaluation of the interactions between lignite and HDPE has been carried out by comparing the experimental yields of the co-pyrolysis of the mixture lignite/HDPE and the theoretical (calculated) yields = (yield of lignite + yield HDPE)/2 (Table VII). At the temperature of 400 °C the experimental and calcul-

TABLE VII. Comparison of the experimental yields of the co-pyrolysis of the mixture lignite/HDPE and theoretical (calculated) yields

Yield <i>t</i> / °C	Lignite/HDPE mixture (experimental)			Lignite/HDPE mixture (theoretical) <sup>a</sup>			Difference (experimental yield – theoretical yield)		
	Liquid, %	Gas, %	Solid, %	Liquid, %	Gas, %	Solid, %	Liquid, %	Gas, %	Solid, %
400	7.49	11.37	81.14	7.04	11.71	81.25	0.45	-0.34	-0.11
450	15.79	21.08	63.13	11.26	15.66	73.08	4.53	5.42	-9.95
500	23.95	40.01	36.04	17.57	17.92	64.51	6.38	22.09	-28.47

<sup>a</sup>Theoretical (calculated) yield = (yield of lignite + yield HDPE)/2; yields of the products of HDPE and lignite pyrolysis are given in Table II

ated yields are very similar, indicating no synergistic effect between lignite and HDPE. This result can be attributed to the thermal stability of HDPE up to 400 °C (Fig. 1). However, at the temperatures of 450 °C and particularly 500 °C, the experimental yields of gas and liquid products are obviously higher than the theoretical ones (Table VII), indicating the synergistic effect between lignite and HDPE. At both temperatures 450 and 500 °C where synergistic effect was observed, the difference between the experimental yields and calculated yields is higher for gaseous than for liquid products. This result is consistent with the predominance of type III kerogen in lignite, which has higher gaseous than liquid hydrocarbon generation potential.<sup>20,25</sup>

#### CONCLUSION

The pyrolysis of HDPE in the open system yielded liquid (oil), gas, and solid residue. Rise of the temperature from 400 to 500 °C resulted in the increase of conversion of HDPE into liquid and gaseous products.

The isotopic compositions of the pyrolysis products indicate that pyrolysis of HDPE in the open system follows the order of degradation of carbon–carbon bonds in natural conditions.

The main constituents of all liquid pyrolysates are terminal *n*-alkenes, *n*-alkanes and terminal *n*-dienes. They were identified in range from C<sub>12</sub> to C<sub>43</sub>. *n*-Alkylcyclohexanes are observed in very low amount, confirming the cyclisation of reactive radicals. *n*-Alkylbenzenes and *n*-alkyltoluenes were identified in trace amounts, which documents that the secondary processes are avoided in the open pyrolysis system. The rise of pyrolysis temperature resulted in the increase contents of mid- and short-chain homologues, in the distributions of all mentioned hydrocarbons. The increase of pyrolysis temperature is associated with the increased content of *n*-dienes and lower content of *n*-alkanes, whereas terminal *n*-alkenes comprise about 50 % of liquid pyrolysate at all temperatures. The pyrolysate obtained at 400 °C is characterised by the prevalence of waxy hydrocarbons, which indicates that under the applied conditions this temperature is not sufficient to produce the liquid pyrolysate, having the composition of *n*-alkanes similar to crude oil. Distribution of *n*-alkanes in pyrolysate at 500 °C is similar to those of crude oil of terrestrial origin.

The obtained results showed that pyrolysis of HDPE in the open system could not serve for direct producing of gasoline or diesel. However, it is useful as a pretreatment to yield a product to be blended into a refinery or petrochemical feed stream. Remarkable environmental characteristic of liquid pyrolysate in comparison to crude oil is extremely low content of aromatic hydrocarbons and absence of asphaltenes and polar compounds.

The gaseous products produced by the pyrolysis of HDPE have desirable composition and consist mainly of methane and ethene. The generation of hydro-

carbon-rich liquid and gaseous products from HDPE can improve the composition of liquid pyrolysates and gases from coal and oil shale by the co-pyrolysis process.

The solid residues showed high calorific values. However, the solid products probably have undesirable combustion behaviour, due to the melting during combustion. Therefore their mixing with coal or biomass is suggested. The mixing of solid residues with coal/biomass for combustion process has advantage, since the solid materials obtained by HDPE pyrolysis do not contain sulphur and do not produce ash by combustion.

The co-pyrolysis of HDPE with mineral-rich lignite indicated the positive synergetic effect at 450 and 500 °C, which is reflected through the increased experimental yields of liquid and gaseous products in comparison to the theoretical ones.

#### SUPPLEMENTARY MATERIAL

Additional information and total ion current of liquid pyrolysates are available electronically at the pages of journal website: <http://www.shd.org.rs/JSCS/>, or from the corresponding author on request.

*Acknowledgement.* The study was financed by the Ministry of Education, Science and Technological Development of the Republic of Serbia (Projects 176006 and 451-03-01039/2015-09/05) and Österreichischer Austauschdienst (OeAD) (Project No. SRB 18/2016) which are gratefully acknowledged. We are also thankful to the reviewers.

#### ИЗВОД

ИСПИТИВАЊЕ ПИРОЛИЗЕ ПОЛИЕТИЛЕНА ВИСОКЕ ГУСТИНЕ У ОТВОРЕНОМ СИСТЕМУ И ПРОЦЕНА ЊЕГОВЕ ПОДОБНОСТИ ЗА КОПИРОЛИЗУ СА ЛИГНИТОМ  
ИВАН КОЈИЋ, ACHIM BECHTEL<sup>1</sup>, FRIEDRICH KITTINGER<sup>2</sup>, НИКОЛА СТЕВАНОВИЋ<sup>3</sup>, МАРКО ОБРАДОВИЋ<sup>4</sup>  
и КСЕНИЈА СТОЈАНОВИЋ<sup>3</sup>

Универзитет у Београду, Иновациони центар Хемијској факултети, Студенчески трг 12–16, 11000 Београд, <sup>1</sup>Montanuniversität Leoben, Department of Applied Geosciences and Geophysics, Peter Turner Strasse 5, A-8700 Leoben, Austria, <sup>2</sup>Montanuniversität Leoben, Department of Product Engineering, Franz-Josef-Strasse 18, A-8700 Leoben, Austria, <sup>3</sup>Универзитет у Београду, Хемијски факултет, Студенчески трг 12–16, 11000 Београд и <sup>4</sup>Универзитет у Београду, Машински факултет, Краљице Марије 16, 11000 Београд

Проучавана је пиролиза полиетилена високе густине (high density polyethylene, HDPE) у отвореном систему. Као изврш HDPE коришћена је пластична кеса за паковање хране. Пиролиза је изведена на температурама 400, 450 и 500 °C које су одобрале на основу резултата термогравиметријске анализе. Пиролизом HDPE добијени су течни, гасовити и чврсти производи. Пораст температуре резултовао је повећаном конверзијом HDPE у течне и гасовите производе. Главни састојци течних пиролизата су 1-*n*-алкени, *n*-алкани и терминални *n*-диени. Састав течних пиролизата показује да изведене пиролизе HDPE не могу послужити као једини процес за директно добијање бензина или дизела, већ првенствено као предтређман за добијање производа који би се мешали са нафтом у рафинеријама, или се користили као петрохемијске сировине. Предност течних пиролизата у односу на сирову нафту је изузетно низак садржај ароматичних угљоводоника и одсуство поларних једињења. Гасовити производи пиролизе имају поже-

љан састав и садрже претежно метан и етен. Чврсти остати добијени пиролизом HDPE не стварају пепео при сагоревању и имају високу топлотну моћ. Копиролиза HDPE са земљастим литотипом лигнита на 450 и 500 °C указала је на позитиван синергетски ефекат, који се одражава кроз повећане експерименталне приносе течних и гасовитих производа у поређењу са теоријским.

(Примљено 15. децембра 2017, ревидирано 6. фебруара, прихваћено 9. фебруара 2018)

#### REFERENCES

1. S. Kumar, R. K. Singh, *Braz. J. Chem. Eng.* **28** (2011) 659
2. S. Kumar, A. K. Panda, R. K. Singh, *Resour., Conserv. Recycl.* **55** (2011) 893
3. P. N. Sharratt, Y. H. Lin, A. A. Garforth, J. Dwyer, *Ind. Eng. Chem. Res.* **36** (1997) 118
4. J. W. Park, J. H. Kim, G. Seo, *Polym. Degrad. Stab.* **76** (2002) 495
5. S. Ali, A. A. Garforth, D. H. Harris, D. J. Rawlence, Y. Uemichi, *Catal. Today* **75** (2002) 247
6. A. Aboulkas, T. Makayssi, L. Bilali, K. El Harfi, M. Nadifyine, M. Benchanaa, *Fuel Process. Technol.* **96** (2012) 209
7. S. Matali, N. A. Rahman, S. S. Idris, A. B. Alias, M. R. Mohatar, *J. Teknol.* **76** (2015) 21
8. J. Cai, Y. Wang, L. Zhou, Q. Huang, *Fuel Process. Technol.* **89** (2008) 21
9. S. Melendi-Espina, R. Alvarez, M. A. Diez, M. D. Casal, *Fuel Process. Technol.* **137** (2015) 351
10. L. Ballice, *Fuel Process. Technol.* **86** (2005) 673
11. M. Sert, L. Ballice, M. Yüksel, M. Sağlam, *Oil Shale* **26** (2009) 463
12. H. Pakdel, C. Roy, W. Kalkreuth, *Fuel* **78** (1999) 365
13. N. Vuković, D. Životić, J. G. Mendonça Filho, T. Kravić-Stevović, M. Hámor-Vidó, J. de Oliveira Mendonça, K. Stojanović, *Int. J. Coal Geol.* **154–155** (2016) 213
14. G. Đ. Gajica, A. M. Šajnović, K. A. Stojanović, M. D. Antonijević, N. M. Aleksić, B. S. Jovančićević, *J. Serb. Chem. Soc.* **82** (2017) 1461
15. V. V. Antić, M. P. Antić, A. Kronimus, K. Oing, J. Schwarzbauer, *J. Anal. Appl. Pyrolysis* **90** (2011) 93
16. V. V. Antić, M. P. Antić, A. Kronimus, J. Schwarzbauer, *Hem. Ind.* **66** (2012) 357
17. N. A. al Sandouk-Lincke, J. Schwarzbauer, V. Antić, M. Antić, J. Caase, S. Grünelt, K. Reßing, R. Littke, *Org. Geochem.* **88** (2015) 17
18. S. Khedri, S. Elyasi, *Polym. Degrad. Stab.* **129** (2016) 306
19. D. Mitrović, N. Đoković, D. Životić, A. Bechtel, A. Šajnović, K. Stojanović, *Int. J. Coal Geol.* **168** (2016) 80
20. N. Đoković, D. Mitrović, D. Životić, D. Španić, T. Troskot-Čorbić, O. Cvetković, K. Stojanović, *J. Serb. Chem. Soc.* **80** (2015) 575
21. D. Životić, K. Stojanović, I. Gržetić, B. Jovančićević, O. Cvetković, A. Šajnović, V. Simić, R. Stojaković, G. Scheeder, *Int. J. Coal Geol.* **111** (2013) 5
22. G. H. Taylor, M. Teichmüller, A. Davis, C. F. K. Diessel, R. Littke, P. Robert, *Organic Petrology*, Gebrüder Borntraeger, Berlin, 1998
23. L. J. Thomas, *Coal Geology*, John Wiley & Sons, Ltd, Chichester, 2002
24. M. Kutz, *Handbook of Environmental Degradation of Materials*, 2<sup>nd</sup> ed., Elsevier Inc., Oxford, 2012
25. B. P. Tissot, D. H. Welte, *Petroleum Formation and Occurrence*, 2<sup>nd</sup> ed., Springer-Verlag, Heidelberg, 1984
26. J. A. González-Pérez, N. T. Jiménez-Morillo, J. M. de la Rosa, G. Almendros, F. J. González-Vila, *J. Chromatogr., A* **1388** (2015) 236

27. E. E. Bray, E. D. Evans, *Geochim. Cosmochim. Acta* **22** (1961) 2
28. K. E. Peters, C. C. Walters, J. M. Moldowan, *The Biomarker Guide, Volume 1: Biomarkers and Isotopes in the Environment and Human History*. Cambridge University Press, Cambridge, 2005
29. A. Kostić, *Thermal evolution of organic matter and petroleum generation modelling in the Pannonian basin (Serbia)*, Faculty of Mining and Geology, Belgrade, 2010 (in Serbian)
30. J. A. Onwudili, N. Insura, P. T. Williams, *J. Anal. Appl. Pyrolysis* **86** (2009) 293
31. C. A. Wilkie, *Polym. Degrad. Stab.* **66** (1999) 301
32. S. Singh, C. Wu, P. T. Williams, *J. Anal. Appl. Pyrolysis* **94** (2012) 99
33. M. Arias, I. Penichet, F. Ysambertt, R. Bauzab, M. Zougagh, Á. Ríos, *J. Supercrit. Fluids* **50** (2009) 22
34. S. Hosokai, K. Matsuoka, K. Kuramoto, Y. Suzuki, *Fuel Process. Technol.* **152** (2016) 399
35. A. Demirbaş, *Energy Convers. Manage.* **42** (2001) 183
36. H. H. Lowry, *Chemistry of Coal Utilization, Vol. I*, John Wiley & Sons Inc., New York, 1947
37. F. Schuster, *Brennst.-Chem.* **25** (1934) 45
38. E. S. Grummel, I. Davies, *Fuel* **12** (1933) 199
39. J. Han, X. Yao, Y. Zhan, S-Y. Oh, L-H. Kim, H-J. Kim, *J. Energy Inst.* **90** (2017) 331
40. K. Annamalai, J. Sweeten, S. Ramalingam, *Trans. ASAE* **30** (1987) 1205
41. S. Kathiravale, M. N. M. Yunus, K. Sopian, A. Samsuddin, R. Rahman, *Fuel* **82** (2003) 1119
42. D. A. Tsiamis, M. J. Castaldi, *Determining accurate heating values of non-recycled plastics (NRP)*, Earth Engineering Center City, University of New York, New York, 2016
43. Environment & Plastics Industry Council (EPIC) a council of the Canadian Plastics Industry Association (CPIA), *A Review of the Options for the Thermal Treatment of Plastics*, CPIA, Mississauga, Ontario, 2004
44. N. J. Themelis, M. J. Castaldi, J. Bhatti, L. Arsova, *Energy and economic value of non-recycled plastics (NRP) and municipal solid wastes (MSW) that are currently landfilled in the fifty states*, Earth Engineering Center, Columbia University, New York, 2011
45. Fuels higher calorific values, <http://www.eisco.co/burner/fuels%20higher%20calorific%20values.pdf> (last accessed February 5, 2018)
46. S. L. Wong, N. Ngadi, T. A. T. Abdullah, I. M. Inuwa, *Renewable Sustainable Energy Rev.* **50** (2015) 1167.